

Insight into Group 4 Metallocenium-Mediated Olefin Polymerization Reaction Coordinates Using a Metadynamics Approach

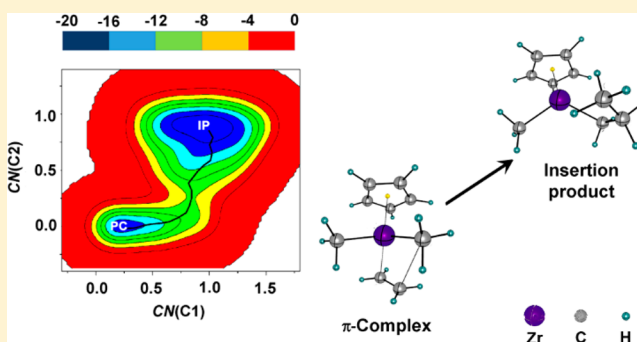
Alessandro Motta,^{*,†} Ignazio L. Fragalà,[†] and Tobin J. Marks^{*,‡}

[†]Dipartimento di Scienze Chimiche, Università di Catania, and INSTM, Udr Catania, Viale A. Doria 6, 95125 Catania, Italy

[‡]Department of Chemistry, Northwestern University, Evanston, Illinois 60208-3113, United States

S Supporting Information

ABSTRACT: We report here the first application of the computationally efficient metadynamics approach for analyzing single-site olefin polymerization mechanisms. The mechanism of group 4 metallocenium catalysis for ethylene homopolymerization is investigated by modeling the ethylene insertion step at the cationic $(\eta^5\text{-C}_5\text{H}_5)\text{Zr}(\text{CH}_3)_2^+$ center using molecular dynamics simulations within the Density Functional Theory (DFT) framework. In particular, the metadynamics formalism is adopted to enable theoretical characterization of covalent bond forming/breaking processes using molecular dynamics ab initio tools. Analysis of the ethylene insertion step free energy surface indicates a slightly exoergic process (-3.2 kcal/mol) with a barrier of 8.6 kcal/mol, in good agreement with conventional ab initio static calculations. Analysis of the structural and dynamic aspects of the simulated reaction coordinate reveals a preferred olefin configuration which aligns parallel to the $\text{Zr}-\text{CH}_3$ vector in concert with insertion and a slightly bent conformation of the product n -propyl chain to avoid nonbonded repulsion between methylene groups. It is found that the unsaturated/electrophilic $\text{CpZr}(\text{CH}_3)_2^+$ center drives the insertion step, thus promoting the formation of the Zr -alkyl bond. The metadynamics analysis uniquely encompasses all energetically possible reaction coordinates, thus providing a more detailed mechanistic picture. These results demonstrate the potential of metadynamics in the conformational and geometrical analysis of transition metal-centered homogeneous catalytic processes.



INTRODUCTION

The past several decades have witnessed great scientific and technological interest in the insertive polymerization of olefins by molecule-based early transition metal catalysts.¹ Here, understanding the intricate structure–reactivity interplay in these homogeneous catalytic systems remains a central issue for the optimal design of novel catalysts and product polymer architectures. In this general scenario, group 4 metallocenium olefin polymerization catalysts have been shown to exhibit very high activities and precise control over product macromolecular architectures, thereby stimulating intense worldwide basic and applied research efforts.² The generally accepted mechanism for single-site olefin polymerization (Cossee–Arlman)³ involves olefin coordination to/activation at a vacant catalytic site (π -complex), followed by alkyl migration of the σ -coordinated polymeryl chain to the activated, π -coordinated olefin as shown in Scheme 1. Here the course of the catalytic process, including the propagation activity, regio- and stereoselectivity, comonomer enchainment selectivity, the interplay between propagation and chain transfer rates, and events controlling polydispersity are highly dependent on the orientation of the monomer relative to the catalyst active site during the insertion step and on the related kinetics. Clearly, those mechanistic factors that govern the ethylene molecule – catalytically active

site interaction remain a central point for completely understanding single-site polymerization processes.

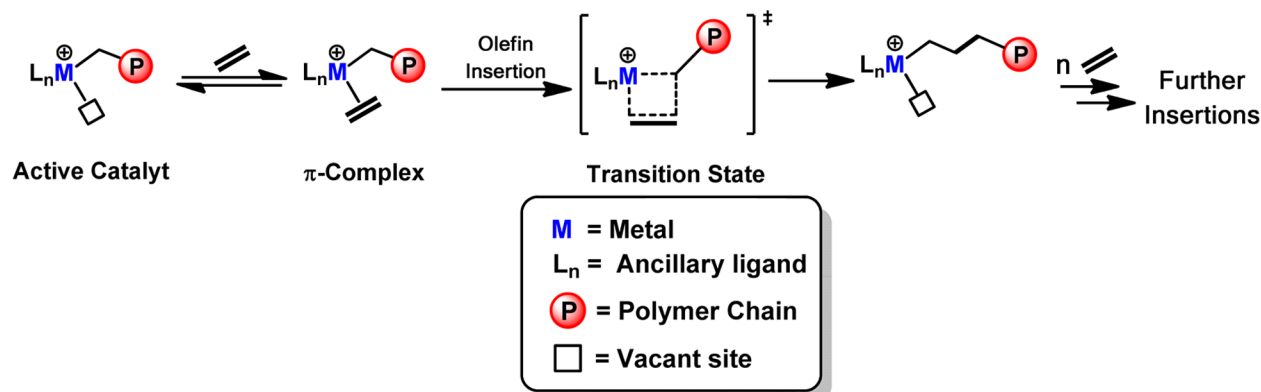
Here theoretical modeling offers an invaluable tool for investigating the sequence of mechanistic events governing the olefin polymerization pathway, and complement purely experimental approaches which are challenged by the intrinsic difficulties of probing such highly labile and sensitive systems.⁴ Therefore, computational approaches represent an essential underpinning of any experimental catalytic effort.⁵ To better understand these processes, quantum chemical attention has focused on propagation mechanisms, on metal identity effects, on ancillary ligand effects,⁶ on counteranion and solvation effects,⁷ and on the kinetics, thermodynamics, and selectivity associated with chain propagation and transfer.

A powerful tool for understanding the behavior of evolving molecular systems in terms of both reactivity and stability lies in the analysis of the underlying free energy landscape. Accurate understanding of this surface offers a similarly accurate description of reaction pathways for chemical reactions as well as the preferred structural configurations of reagents and products. To this end, Molecular Dynamics (MD) has become a standard technique in many branches of science, from physics

Received: March 29, 2013

Published: June 27, 2013

Scheme 1. Ethylene Activation and Enchainment Pathway According to the Cossee–Arman Mechanism



to biology and materials science,^{8–11} reflecting, among other factors, the great recent progress in both low- and high-end computing. Nevertheless, MD simulation results are of significance for free energy landscapes only if the probing is sufficiently elaborate to sample all the energetically relevant configurations of the system (ergodic in the time scale of the simulation). Today the requirements to obtain sufficient statistics require impractically large computational resources.

Metadynamics,¹² a MD-based technique, enhances the sampling of configuration phase space in simulations for estimating free energy landscapes and, hence, is an attractive approach for processes in which changes in electronic structure play a dominant role, namely chemical reactions. These processes can be described with first principles “ab initio MD”, and ab initio-based metadynamics allows traversing chemical transition states which are typically 1 or 2 orders of magnitude greater in energy than $k_B T$ at room temperature. In a reasonable simulation time scale, it has proven to be a powerful recipe for determining the free energy barriers and the lowest free energy pathways of concerted reactions.¹³ To date, studies of chemical reactions using metadynamics techniques have included gas phase¹⁴ and condensed phase¹⁵ reactions, surface chemistry,¹⁶ enzymatic processes,¹⁷ homogeneous,¹⁸ and heterogeneous¹⁹ catalysis.

In general, when the system size and the theoretical approximation level allow dynamic studies of the energetics of a system of interest, the metadynamics approach offers unquestionable attractions compared to static theoretical methods. The principal drawback of the static ab initio approach is that the search for the lowest energy minimum on the potential energy surface can be tedious and somewhat ambiguous for structurally mobile systems having many possible configurations and many possible minima. Indeed, the inherent 0 K temperature associated with the search for the minima on a potential energy surface represents a crude approximation for conformationally flexible systems which can be stereochemically dynamic at finite temperatures. Moreover, after geometry optimizations of minima and transition states, estimation of the Hessian matrices, from which the vibrational contributions to the entropy and the enthalpy are derived, requires a second computing step for both minima and transition state structures, including additional approximations—either harmonic or anharmonic approaches.

All these considerations reflect the many issues associated with static theoretical approaches applied to catalytic reactions and more specifically, to the Cossee–Arman mechanism. Note that in this case the olefin orientation in the π -complex and

growing chain conformation in the insertion product are susceptible to dynamic variations even at room temperature. Note also that in general the most populated (probable) conformations at finite temperature are unlikely to correspond to the geometries at the well bottoms identified in static calculations. Moreover, transition state searches suffer from necessary approximations regarding the related vibrational analysis options (harmonic-anharmonic approaches).

In this perspective, the present paper presents the first application of the metadynamics approach to the analysis of single-site olefin polymerization mechanisms. Attention is focused on the geometric and energetic pathways along the ethylene insertion reaction coordinate involving the model $\text{CpZr}(\text{CH}_3)_2^+$ system, which is highly active for catalytic benzene hydrogenation and ethylene polymerization.²⁰ The results obtained here with the metadynamics formalism are compared and contrasted with both traditional static ab initio methods.

■ COMPUTATIONAL DETAILS

Metadynamics. Molecular catalyst–ethylene interactions were modeled with a DFT periodic approach using the Gaussian and plane wave mixed-basis method, as implemented in the QUICKSTEP module²¹ within the CP2K simulation package.²² A double-quality DZV Gaussian basis set was employed for the Zr atom, and a triple-quality TZVP Gaussian basis set was employed for all the other atoms. The Goedecker–Teter–Hutter pseudopotentials²³ together with a 400 Ry plane wave cutoff were used to expand the densities obtained with the Perdew–Burke–Ernzerhof (PBE)²⁴ exchange–correlation density functional. Dispersion forces are taken into account using the Grimme DFT-D3 Method.²⁵ The free energy landscape is obtained using a metadynamics approach that is based on a dimensional reduction: it requires a previous definition of a set of degrees of freedom, often referred to as collective variables (CVs), describing all the relevant modifications (reaction coordinates) of the process under study. CVs can be distances, angles, dihedral, coordination numbers, or more complicated functions of coordinates. During a MD simulation, small Gaussian-like repulsive potentials (hills) are introduced with a defined frequency on the explored regions of the CV space, thereby disfavoring the system from revisiting already sampled points so that it accelerates “rare” events (long time scale events) arising, for example, from high energetic barriers between two configurations, and maps the free energy surface of the process being simulated. To obtain an overall free energy

surface for the ethylene insertion step into the Zr–CH₃ bond of CpZr(CH₃)₂⁺, we initially used two different collective variables, termed here CV₁ and CV₂. Specifically, CV₁ specifies the coordination number (CN) of the ethylene carbon atoms with respect to bond formation at the Zr center. The other collective variable CV₂ specifies the coordination number of the ethylene carbon atoms with respect to bond formation with one methyl group of the Zr complex.

Metadynamics runs were carried out using Gaussian-shaped potential hills with a height of 1.0 kcal/mol and a width of 0.05 Bohr. The hills were spawned at intervals of 50 fs of MD. To restrict the surface of exploration, an upper limit in both CV₁ and CV₂ was imposed with activation of a quadratic wall positioned at 5.0 Å, with a quadratic potential constant of 40.0 kcal/(mol Å²). Metadynamics were conducted in the NVT ensemble. The temperature was set to 298 K, and each degree of freedom was controlled via a canonical sampling through velocity rescaling with a time constant of 10 fs. Temperature stability was monitored throughout the metadynamics run (see the Supporting Information). A single integration time step of 0.5 fs was used. The runs were protracted for ~16 ps until they exhibited a free diffusivity along the CVs. These convergence criteria were chosen in agreement with the guidelines published in a recent paper assessing the accuracy of metadynamics.²⁶ Trajectories were saved every 10 steps (5 fs time interval) of metadynamics for subsequent analysis. The long MD simulation times guaranteed an extensive sampling of the configurational space, important for providing meaningful determination of the energetics for catalytic reactions.

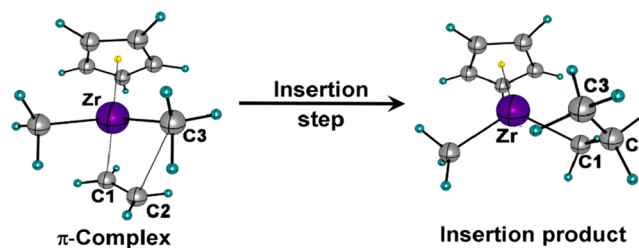
Comparative Static *ab Initio* Calculations. Static calculations were performed using G09.²⁷ Calculations were performed at the level of the PBE formalism for both exchange and correlation functionals. The effective core potential (ECP) of Hay and Wadt,²⁸ which explicitly treats 4s and 4p electrons and a basis set contracted as [4s, 4p, 4d], were used for the zirconium atom. The standard all-electron 6-31G** basis was used for the remaining atoms.²⁹ Dispersion forces are taken into account as implemented in the code. Molecular geometry optimization of stationary points used analytical gradient techniques. The transition state was searched using the synchronous, transit-guided quasi-Newton method.³⁰ Frequency analyses were performed to obtain thermochemical information about the reaction pathways at 298 K in the harmonic approximation. The force constants were determined analytically. All calculations (metadynamics and static) ran on CINECA PLX cluster.

RESULTS AND DISCUSSION

In this section, we discuss a metadynamics analysis of the insertion step of a prototypical olefin at an organozirconium catalytic center activated for olefin polymerization. The conformational aspects associated with the stable intermediates (π -complex and kinetic products) are scrutinized, and their geometrical evolution along the insertion reaction coordinate is analyzed in detail. The mechanistic picture emerging from this analysis is then compared and contrasted with the standard static *ab initio* approach.

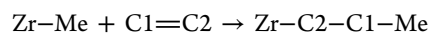
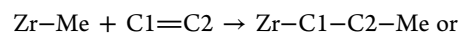
To probe all mechanistic issues at the molecular level, we first reconstructed the free energy surfaces (FESs) for the ethylene insertion step into a Zr–CH₃ bond of the prototypical (η^5 -C₅H₅)Zr(CH₃)₂⁺ cation. The choice of collective variables is crucial for the successful application of a metadynamics simulation. From Scheme 2, the fundamental geometrical

Scheme 2. Representative Snapshots of the Ethylene π -Complex at the Cationic (η^5 -C₅H₅)Zr(CH₃)₂⁺ Catalyst and the Ethylene Insertion Product during the Molecular Dynamics



variables describing the insertion process are represented by the distances between the atoms directly involved in the 4-center olefin insertion process. During this step, both $r(\text{Zr}-\text{C1})$, the distance between the Zr center and one ethylene C atom, and $r(\text{C2}-\text{C3})$, the distance between one catalyst CH₃ group and the other carbon atom of the inserting ethylene, decrease in concert with the formation of the two new sigma bonds. In contrast, the ethylene C=C double bond distance, $r(\text{C1}-\text{C2})$, elongates to a single bond distance, while the Zr–CH₃ bond $r(\text{Zr}-\text{C3})$ is lost due to the olefin insertion. In this context, several possible CVs can be chosen to analyze the ethylene insertion step.

One of the most efficient CVs for probing changes is the coordination number (CN) of the two carbon atoms of ethylene. Hence, to reduce the complexity while maintaining an accurate description of the system, two CVs were chosen and defined as CN1 and CN2. Here CN1 accounts for the Zr–C1 bond formation, while CN2 describes the emerging C2–C3 bond along the insertion reaction coordinate (Scheme 2). Note that the coordination number (CN) is intended as a descriptor of ethylene carbon atom connectivity either with respect to bonding to the Zr center (CN1) or to the methyl group (CN2). This choice introduces the least number of constraints because it does not interfere with the intrinsic mobility of the ethylene molecule that, in turn, can insert into the Zr center in either orientation:



The Free Energy Surface (FES) is projected along these two CVs, and the energetic results describing Scheme 2 are shown in Figure 1. The FES exhibits two broad minima corresponding to the ethylene π -complex and to the ethylene insertion product. The reaction is found to be slightly exothermic, and the total free energy change, extrapolated from the values reported in Figure 1, is $\Delta G = -3.2 \pm 1$ kcal/mol. Based on both experiment² and theory,⁴ literature data suggest that the reaction proceeds from the PC to the IP through an alkyl migration of the σ -coordinated growing chain to the π -coordinated olefin. The TS structure involves a coplanar arrangement of the Zr–Me vector and the double bond with a ΔG^\ddagger variation of 8.6 ± 1 kcal/mol. From the energy contour plot (Figure 1b) there is evidence that at the transition state, the Zr–C1 bond is almost completely formed (CN1 \approx 0.8), while the C2–C3 bond is still emerging (CN2 \approx 0.3). Note that even though this enchainment step is a concerted bond forming/breaking process, the present result indicates that the unsaturated/electrophilic CpZr(CH₃)₂⁺ center drives the

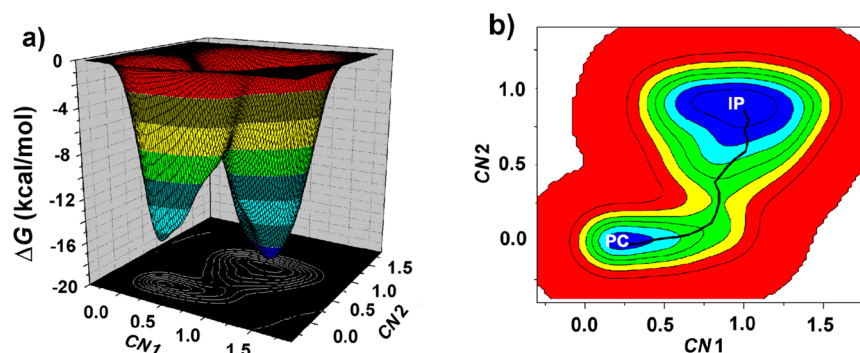


Figure 1. A. Reaction free energy surface and B. Energetic contour plot of the ethylene insertion step into a Zr–CH₃ bond of the catalyst in Scheme 2, reconstructed using metadynamics as a function of two CVs, specifically, CN1 and CN2. Free energy is in kcal/mol; the reaction pathway from the π -complex (PC) to the insertion product (IP) is visualized with a solid line.

insertion step, thus promoting the formation of the Zr–alkyl bond.

In Figure 2, the time evolution of the key distances involved in the olefin insertion step are displayed together with the times

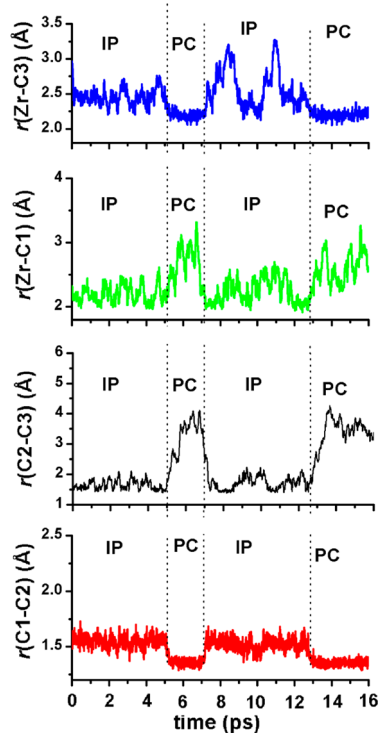


Figure 2. Time evolution of key distances involved in the ethylene + CpZr(CH₃)₂⁺ insertion step during a metadynamics run. Vertical lines give the time at which reaction takes place. IP = insertion product, PC = π -complex.

at which the insertion step and the reverse reaction occur. The observation of the “retro” process restoring the reagent species highlights the early achievement of free diffusivity conditions along the CVs. Since the time reversibility of the motion equation is used in metadynamics, the starting geometry is not crucial. In the present treatment, the simulation begins from the insertion product. Scrutinizing the time evolution of all the aforementioned variables reveals a step at about 5 ps and one at about 13 ps corresponding to the principal atomic displacements associated with the insertion step. These results are

evident in the elongation of the olefin C=C bond from 1.33 Å to 1.54 Å to form a C–C single bond and by the contraction of the Zr–C1 bond to 2.32 Å as a consequence of the Zr–alkyl bond formation. Moreover, single bond formation between the olefin C2 atom and the methyl C3 in the insertion product is confirmed by the C2–C3 distance (Figure 2) of 1.54 Å. In the π -complex, the C2–C3 distance is susceptible to large excursions as expected for initially noninteracting atoms. An opposite trend is found for the Zr–C3 distance, since the bond is formed in the π -complex (2.32 Å) and lost in the insertion product.

It is also informative to examine trends in the Zr–C1–C2–C3 dihedral angle (Figure 3). This trend finds a counterpart in the possible rotation of the π -complexed ethylene about the Zr–ethylene centroid axis and in a similar rotation of the *n*-propyl chain of the insertion product about the C1–C2 bond. Such an analysis can reveal preferential orientations of either the π -complexed olefin molecules or the growing polymer chain with respect to the catalyst active site. From statistical analysis of all configurations along the trajectory, a preferred parallel orientation of the ethylene relative to the Zr–Me bond emerges in the PC, while high conformational mobility of the *n*-propyl chain is observed in the IP. Finally, the variations of all the geometrical parameters shown in Figures 2 and 3 are synchronous as a consequence of the concerted bond-forming/-breaking process.

Thermochemical Analysis from Static *ab Initio* Computation. A comparison of the thermochemical analysis based on the present molecular dynamic evaluation with that computed using the standard, static *ab initio* (0 K) approach is informative in validating the present results as well as in confirming the present metadynamics analysis as a suitable theoretical methodology for investigating the thermochemical and kinetic properties of transition metal-centered catalytic processes. The structures of the reagent and product optimized by the static calculation converge to geometries very similar to those derived from the metadynamics analysis. Note, however, that static calculations converge to only one configuration for a stable intermediate (π -complex) and insertion product, while the metadynamics treatment takes into account a wide range of either π -complex or insertion product configurations compatible with the finite temperature (*vide supra*). Figure 4 summarizes the energetic profiles of the olefin insertion step in terms of Gibbs free energy derived from both static and metadynamics calculations. Stabilization on passing from π -complex to insertion product as well as the insertion kinetic

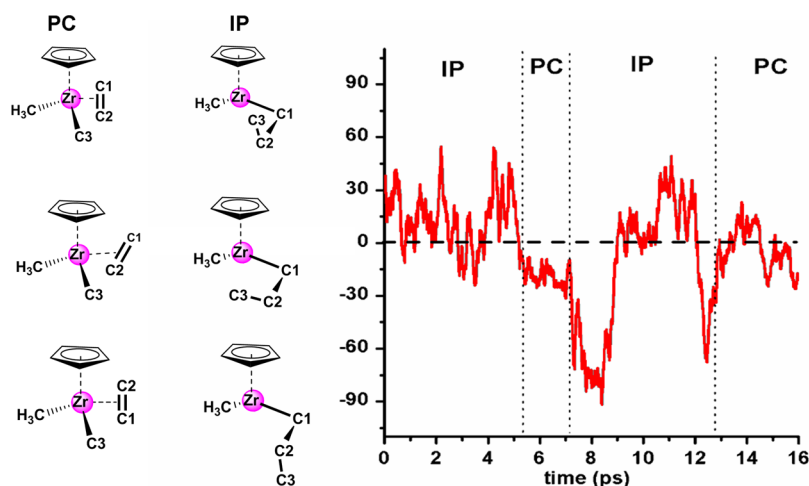


Figure 3. Time evolution of the Zr–C1–C2–C3 dihedral angle during a metadynamics run. Vertical dotted lines indicate the time at which the enchainment reaction takes place. IP = insertion product, PC = π -complex.

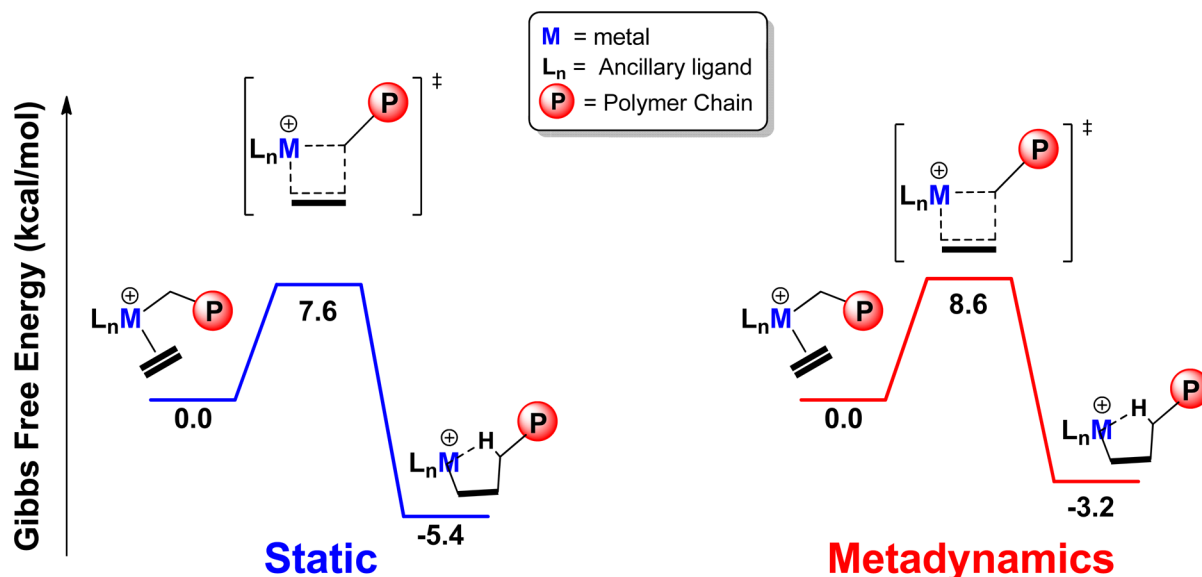


Figure 4. Computed Gibbs free energies of species on the ethylene insertion pathway at the $(\eta^5\text{-C}_5\text{H}_5)\text{Zr}(\text{CH}_3)_2^+$ cation computed by the static and metadynamic approaches (kcal/mol).

barrier computed with the ab initio static approach are comparable to that computed with metadynamics. Note also that the free energy difference between the π -complex and the insertion product is -5.4 kcal/mol and that the free energy barrier is 7.6 kcal/mol value by the static approach. These results are very similar to those extracted from the metadynamics approach. Moreover, all these energetic data are consistent with different static approximations (Table S1) and with previous calculations regarding olefin insertion in the parent metallocene catalyst.¹⁵ Finally, the IRC path has been computed, and CN1 and CN2 have been evaluated along the entire pathway (Figure 5). At the transition state, we have found values of 0.56 and 0.04 for CN1 and CN2, respectively, perfectly in tune with the trends found from the MD approach (vide supra). This result represents a further validation of the MD approach as a reliable tool in the investigation of catalytic processes

In this general context, the information emerging here is that the search for the lowest energy minimum on the potential energy surface performed by the ab initio static approach can be

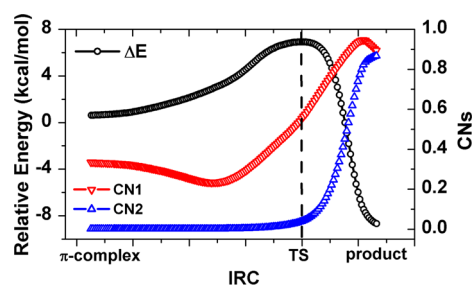


Figure 5. IRC pathway and CN collective variables computed with the static approach along the insertion step.

incomplete or at least ambiguous when conformationally mobile systems having many possible configurations and many possible energetic minima are involved. In fact, the inherent 0 K temperature associated with the search for the minima on the potential energy surface represents a crude approximation for conformationally mobile systems which can be stereochemically dynamic at finite temperatures. Moreover,

after geometry optimizations of minima and transition states, and estimation of the Hessian matrices from which the vibrational contributions to the entropy and the enthalpy are derived, a second computational step is required for both minima and transition state structures, including additional approximations, specifically harmonic or anharmonic approaches. In contrast, metadynamics simulations provide thermochemical and kinetic information at finite temperatures where the results can be compared with experiment, typically performed near room temperature. At finite temperatures, there can be a conformational equilibration between different isomeric conformations.

In the present example, all the conformations populated on traversing the potential energy surface are taken into account in the energetic and geometric analysis of the catalytic process. This approach is particularly relevant in this study for the many possible conformations of the olefin π -complex (vide supra). Note that in general the most populated (probable) conformations at finite temperature cannot correspond to the geometries at the well bottoms identified in static calculations. In the case of the present π -complex, static calculations only take into account a single possible conformation, neglecting all the other possible orientations accessible at finite temperatures. These considerations render dynamic approaches more realistic in investigating interactions such as those that direct enchainment stereochemistry at the catalytic site and highlight how dynamical approaches can be adopted in addition to the traditional static approaches to obtain a more complete analysis of the catalytic processes under investigation.

CONCLUDING REMARKS

The catalytic activity of a prototypical metallocenium complex toward olefin polymerization has been investigated for the first time using a molecular dynamics tool based on DFT. Specifically, the conformational and energetic aspects of the ethylene insertion step at the cationic $\text{CpZr}(\text{CH}_3)_2^+$ catalyst have been scrutinized via a metadynamics analysis. It is found that the insertion step is essentially thermoneutral ($\Delta G = -3.2$ kcal/mol), with an energetic barrier of 8.6 kcal/mol. From the free energy landscape it is evident that the unsaturated Zr center facilitates this process. Moreover, the trends in the geometrical parameters involved in the reaction reveal a concerted but not completely synchronous bond-breaking/forming process. That is, the unsaturated/electrophilic $\text{CpZr}(\text{CH}_3)_2^+$ center drives the insertion step by promoting initial formation of the Zr-alkyl bond. A preferred parallel orientation of the ethylene monomer relative to the Zr-Me bond emerges in the π -complex, while a highly mobile *n*-propyl chain is observed in the insertion product. The present comparison with the conventional static theoretical approach validates the metadynamics analysis as a powerful theoretical tool to investigate transition metal-centered catalytic reactions and highlights some of the added values of Metadynamics with respect to the static approach.

ASSOCIATED CONTENT

Supporting Information

Further details about metadynamics trajectories, details concerning the comparison between the MD approach, and static approaches with different approximations are provided. Moreover optimized geometries in Cartesian coordinates of the stable and transition state structures performed by the static

calculations. This material is available free of charge via the Internet at <http://pubs.acs.org>.

AUTHOR INFORMATION

Corresponding Author

*E-mail: a.motta@dipchi.unict.it.

Notes

The authors declare no competing financial interest.

ACKNOWLEDGMENTS

This research was supported by the Ministero dell'Istruzione, dell'Università e della Ricerca (MIUR Rome) and by U.S. Department of Energy Office of Science, Office of Basic Energy Sciences, under grant DE-FG02-86ER13511. We acknowledge the CINECA Award N. HP10BD82EA, 2011 for the availability of high performance computing resources and support.

REFERENCES

- (1) For recent reviews of this field, see: (a) Nomura, K.; Zhang, S. *Chem. Rev.* **2011**, *111*, 2342–2363. (b) Makio, H.; Terao, H.; Iwashita, A.; Fujita, T. *Chem. Rev.* **2011**, *111*, 2363–2449. (c) Delferro, M.; Marks, T. J. *Chem. Rev.* **2011**, *111*, 2450–2485. (d) Takeuchi, D. *Dalton Trans.* **2010**, 39, 311–328. (e) Nakamura, A.; Ito, S.; Nozaki, K. *Chem. Rev.* **2009**, *109*, 5215–5244. (f) Chen, E. Y. X. *Chem. Rev.* **2009**, *109*, 5157–5214. (g) Hustad, P. D. *Science* **2009**, *325*, 704–707. (h) Amin, S. B.; Marks, T. J. *Angew. Chem., Int. Ed.* **2008**, *47*, 2006–2025. (i) Marks, T. J. *Proc. Natl. Acad. Sci. U.S.A.* **2006**, *103*, 15288–15354. (j) Zhang, J.; Wang, X.; Jin, G. X. *Coord. Chem. Rev.* **2006**, *250*, 95–109. (k) Durand, J.; Milani, B. *Coord. Chem. Rev.* **2006**, *250*, 542–560. (l) Delacroix, O.; Gladysz, J. A. *Chem. Commun.* **2003**, *6*, 665–675. (m) Kaminsky, W.; Arndt-Rosenau, M. *Applied Homogeneous Catalysis with Organometallic Compounds*, 2nd ed.; Wiley-VCH Verlag GmbH: Weinheim, Germany, 2002. (n) Gibson, V. C.; Spitzmesser, S. K. *Chem. Rev.* **2003**, *103*, 283–316. (o) Mecking, S. *Coord. Chem. Rev.* **2000**, *203*, 325–351. (p) Ittel, S. D.; Johnson, L. K.; Brookhart, M. *Chem. Rev.* **2000**, *100*, 1169–1204. (q) Britovsek, G. J. P.; Gibson, V. C.; Wass, D. F. *Angew. Chem., Int. Ed.* **1999**, *38*, 428–447.
- (2) For recent reviews of group 4 based catalysis, see: (a) Bochmann, M. *Organometallics* **2010**, *29*, 4711–4740. (b) Makio, H.; Fujita, T. *Acc. Chem. Res.* **2009**, *42*, 1532–1544. (c) Domski, G. J.; Rose, J. M.; Coates, G. W.; Bolig, A. D.; Brookhart, M. *Prog. Polym. Sci.* **2007**, *32*, 30–92. (d) Suzuki, N. *Top. Organomet. Chem.* **2005**, *8*, 177–216. (e) Alt, H. G. *Dalton Trans.* **2005**, 20, 3271–3276. (f) Kaminsky, W. J. *Polym. Sci., Part A: Polym. Chem.* **2004**, *42*, 3911–3921. (g) Wang, W.; Wang, L. J. *Polym. Mater.* **2003**, *20*, 1–8. (h) Lin, S.; Waymouth, R. M. *Acc. Chem. Res.* **2002**, *35*, 765–773. (i) Chen, E. Y.-X.; Marks, T. J. *Chem. Rev.* **2000**, *100*, 1391–1434. (j) Boffa, L. S.; Novak, B. M. *Chem. Rev.* **2000**, *100*, 1479–1493.
- (3) (a) Cossee, P. J. *Catal.* **1964**, *3*, 80–88. (b) Arlman, E. J.; Cossee, P. J. *Catal.* **1964**, *3*, 99–104.
- (4) (a) Sameera, W. M. C.; Maseras, F. *Wiley Interdiscip. Rev.: Comput. Mol. Sci.* **2012**, *2*, 375–385. (b) Motta, A.; Fragalà, I. L.; Marks, T. J. *J. Am. Chem. Soc.* **2009**, *131*, 3974–3984. (c) Motta, A.; Fragalà, I. L.; Marks, T. J. *J. Am. Chem. Soc.* **2007**, *129*, 7327–7338. (d) Yang, S.-Y.; Ziegler, T. *Organometallics* **2006**, *25*, 887–900. (e) Zurek, E.; Ziegler, T. *Prog. Polym. Sci.* **2004**, *29*, 107–148. (f) Lanza, G.; Fragalà, I. L.; Marks, T. J. *Organometallics* **2002**, *21*, 5594–5612.
- (5) (a) Ciancaleoni, G.; Fraldi, N.; Cipullo, R.; Busico, V.; Macchioni, A.; Budzelaar, P. H. M. *Macromolecules* **2012**, *45*, 4046–4053. (b) Bagh, B.; Schatte, G.; Green, J. C.; Muller, J. J. *Am. Chem. Soc.* **2012**, *134*, 7924–7936. (c) Yang, S.-Y.; Xiang, M.-L.; Chen, L.-J.; Xie, G.-B.; Shi, B.; Wei, Y.-Q.; Ziegler, T. *J. Comput. Chem.* **2007**, *28*, 513–518. (d) Caporaso, L.; Gracia-Budria, J.; Cavallo, L. *J. Am. Chem. Soc.* **2006**, *128*, 16649–16654. (e) Wondimagegn, T.; Xu, Z.; Vanka, K.; Ziegler, T. *Organometallics* **2005**, *24*, 2076–2085. (f) Besedin, D. V.; Ustynyuk, L. Y.; Ustynyuk, Y. A.; Lunin, V. V. *Top. Catal.* **2005**, *32*,

- 47–60. (g) Ujaque, G.; Maseras, F. *Struct. Bonding (Berlin, Ger.)* **2004**, 112, 117–149. (h) Cavallo, L. *Catal. Met. Complexes* **2002**, 25, 23–56.
- (6) (a) Tomasi, S.; Razavi, A.; Ziegler, T. *Organometallics* **2009**, 28, 2609–2618. (b) Zhu, C.; Ziegler, T. *Inorg. Chim. Acta* **2003**, 345, 1–7. (c) Froese, R. D. J.; Musaev, D. G.; Morokuma, K. *Organometallics* **1999**, 18, 373–379. (d) Musaev, D. G.; Froese, R. D. J.; Morokuma, K. *New J. Chem.* **1997**, 21, 1269–1282. (e) Koga, N.; Yoshida, T.; Morokuma, K. *Ziegler Catal. Fink, G., Müllhaupt, R., Brintzinger, H. H., Eds.; Springer: Berlin, Germany, 1995; pp 275–89.*
- (7) (a) Flisak, Z.; Suchorska, P. *Organometallics* **2010**, 29, 6196–6200. (b) Zurek, E.; Ziegler, T. *Prog. Polym. Sci.* **2004**, 29, 107–148. (c) Xu, Z.; Vanca, K.; Ziegler, T. *Macromol. Symp.* **2004**, 206, 457–469. (d) Wondimagegn, T.; Xu, Z.; Vanca, K.; Ziegler, T. *Organometallics* **2004**, 23, 3847–3852. (e) Lanza, G.; Fragalà, I. L.; Marks, T. J. *Organometallics* **2002**, 21, 5594–5612. (f) Xu, Z.; Vanca, K.; Firman, T.; Michalak, A.; Zurek, E.; Zhu, C.; Ziegler, T. *Organometallics* **2002**, 21, 2444–2453. (g) Lanza, G.; Fragalà, I. L.; Marks, T. J. *J. Am. Chem. Soc.* **2000**, 122, 12764–12777. (h) Ystenes, M.; Eilertsen, J. L.; Liu, J.; Ott, M.; Rytter, E.; Stovng, J. A. *J. Polym. Sci., Polym. Chem.* **2000**, 38, 3450.
- (8) (a) Verdolino, V.; Baldini, L.; Palazzesi, F.; Giberti, F.; Parrinello, M. J. *Phys. Chem. C* **2012**, 116, 23441–23452. (b) Martonak, R.; Donadio, D.; Oganov, A. R.; Parrinello, M. *Nat. Mater.* **2006**, 5, 623–626.
- (9) (a) Soderhjelm, P.; Tribello, G. A.; Parrinello, M. *Proc. Natl. Acad. Sci. U. S. A.* **2012**, 109, 5170–5175, S5170/1–S5170/4. (b) Oganov, A.; Martonak, R.; Laio, A.; Raiteri, P.; Parrinello, M. *Nature* **2005**, 438, 1142–1144.
- (10) Sun, J.; Klug, D. D.; Martonak, R.; Montoya, J. A.; Less, M. S.; Scandolo, S.; Tosatti, E. *Proc. Natl. Acad. Sci. U.S.A.* **2009**, 106, 6077–6081.
- (11) Yao, Y.; Klug, D. D.; Sun, J.; Martonak, R. *Phys. Rev. Lett.* **2009**, 103, 055503.
- (12) (a) Barucci, A.; Bonomi, M.; Parrinello, M. *Adv. Rev.* **2011**, 1, 826–843. (b) Iannuzzi, M.; Laio, A.; Parrinello, M. *Phys. Rev. Lett.* **2003**, 90, 238302.
- (13) Ensing, B.; Klein, M. *Proc. Natl. Acad. Sci. U.S.A.* **2005**, 102, 6755–6759.
- (14) (a) Gallet, G. A.; Pietrucci, F.; Andreoni, W. *J. Chem. Theory Comput.* **2012**, 8, 4029–4039. (b) Xiao, S.; Wang, L.; Liu, Y.; Lin, X.; Liang, H. *J. Chem. Phys.* **2012**, 137, 195101/1–195101/8. (c) Shi, T.; Siu, C.-K.; Siu, K. W. M.; Hopkinson, A. C. *Angew. Chem., Int. Ed.* **2008**, 47, 8288–8291.
- (15) (a) Bisha, I.; Laio, A.; Magistrato, A.; Giorgetti, A.; Sgrignani, J. *J. Chem. Theory Comput.* **2013**, 9, 1240–1246. (b) Gronau, G.; Qin, Z.; Buehler, M. J. *Biomater. Sci.* **2013**, 1, 276–284. (c) Liu, H.; Zhu, L.; Cui, W.; Ma, Y. *J. Chem. Phys.* **2012**, 137, 074501/1–074501/7. (d) Angioletti-Uberti, S.; Ceriotti, M.; Lee, P. D.; Finnis, M. W. *Phys. Rev. B: Condens. Matter Mater. Phys.* **2010**, 81, 125416/1–125416/11. (e) Gunaydin, H.; Houk, K. N. *J. Am. Chem. Soc.* **2008**, 130, 15232–15233. (f) Blumberger, J.; Ensing, B.; Klein, M. *Angew. Chem., Int. Ed.* **2006**, 45, 2893–2897.
- (16) (a) Kuo, I. F. W.; Grant, C. D.; Gee, R. H.; Chinn, S. C.; Love, A. H. *J. Phys. Chem. C* **2012**, 116, 9631–9635. (b) Vartak, S.; Roudgar, A.; Golovnev, A.; Eikerling, M. *J. Phys. Chem. B* **2013**, 117, 583–588. (c) Kostov, M.; Santiso, E.; George, A.; Gubbins, K.; Nardelli, M. *Phys. Rev. Lett.* **2005**, 95, 136105.
- (17) (a) Biarnes, X.; Ardevol, A.; Iglesias-Fernandez, J.; Planas, A.; Rovira, C. *J. Am. Chem. Soc.* **2011**, 133, 20301–20309. (b) Boero, M. *J. Phys. Chem. B* **2011**, 115, 12276–12286. (c) Vidossich, P.; Fiorin, G.; Alfonso-Prieto, M.; Derat, E.; Shaik, S.; Rovira, C. *J. Phys. Chem. B* **2010**, 114, 5161–5169. (d) Boero, M.; Ikeda, T.; Ito, E.; Terakura, K. *J. Am. Chem. Soc.* **2006**, 128, 16798–16807.
- (18) Stirling, A.; Iannuzzi, M.; Parrinello, M.; Molnar, F.; Bernhart, V.; Luinstra, G. A. *Organometallics* **2005**, 24, 2533–2537.
- (19) Kiss, J.; Frenzel, J.; Nair, N. N.; Meyer, B.; Marx, D. *J. Chem. Phys.* **2011**, 134, 064710.
- (20) (a) Williams, L. A.; Guo, N.; Motta, A.; Delferro, M.; Fragalà, I. L.; Miller, J. T.; Marks, T. J. *Proc. Nat. Acad. Sci.* **2013**, 110, 413–418.
- (b) Nicholas, C. P.; Marks, T. J. *Langmuir* **2004**, 20, 9456–9462.
- (c) Nicholas, C. P.; Ahn, H.; Marks, T. J. *J. Am. Chem. Soc.* **2003**, 125, 4325–4331.
- (21) VandeVondele, J.; Krack, M.; Mohamed, F.; Parrinello, M.; Chassaing, T.; Hutter, J. *Comput. Phys. Commun.* **2005**, 167, 103–128.
- (22) The CP2K developers group. <http://www.cp2k.org> (accessed Feb 21, 2013).
- (23) Goedecker, S.; Teter, M.; Hutter, J. *Phys. Rev. B* **1996**, 54, 1703.
- (24) Perdew, J. P.; Burke, K.; Ernzerhof, M. *Phys. Rev. Lett.* **1997**, 78, 1396.
- (25) Grimme, S. J.; Antony, J.; Ehrlich, S.; Krieg, H. *Comput. Chem.* **2010**, 132, 154104.
- (26) Laio, A.; Rodriguez-Forte, A.; Gervasio, F. L.; Cecarelli, M.; Parrinello, M. *J. Phys. Chem. B* **2005**, 109, 6714–6721.
- (27) Frisch, M. J.; Trucks, G. W.; Schlegel, H. B.; Scuseria, G. E.; Robb, M. A.; Cheeseman, J. R.; Scalmani, G.; Barone, V.; Mennucci, B.; Petersson, G. A.; Nakatsuji, H.; Caricato, M.; Li, X.; Hratchian, H. P.; Izmaylov, A. F.; Bloino, J.; Zheng, G.; Sonnenberg, J. L.; Hada, M.; Ehara, M.; Toyota, K.; Fukuda, R.; Hasegawa, J.; Ishida, M.; Nakajima, T.; Honda, Y.; Kitao, O.; Nakai, H.; Vreven, T.; Montgomery, J. A., Jr.; Peralta, J. E.; Ogliaro, F.; Bearpark, M.; Heyd, J. J.; Brothers, E.; Kudin, K. N.; Staroverov, V. N.; Kobayashi, R.; Normand, J.; Raghavachari, K.; Rendell, A.; Burant, J. C.; Iyengar, S. S.; Tomasi, J.; Cossi, M.; Rega, N.; Millam, J. M.; Klene, M.; Knox, J. E.; Cross, J. B.; Bakken, V.; Adamo, C.; Jaramillo, J.; Gomperts, R.; Stratmann, R. E.; Yazyev, O.; Austin, A. J.; Cammi, R.; Pomelli, C.; Ochterski, J. W.; Martin, R. L.; Morokuma, K.; Zakrzewski, V. G.; Voth, G. A.; Salvador, P.; Dannenberg, J. J.; Dapprich, S.; Daniels, A. D.; Farkas, Ö.; Foresman, J. B.; Ortiz, J. V.; Cioslowski, J.; Fox, D. J. *Gaussian 09, Revision C.01*; Gaussian, Inc.: Wallingford, CT, 2009.
- (28) Hay, P. J.; Wadt, W. R. *J. Chem. Phys.* **1985**, 82, 299–310.
- (29) (a) Hehre, W. J.; Ditchfield, R.; Pople, J. A. *J. Chem. Phys.* **1972**, 56, 2257–2261. (b) Francl, M. M.; Pietro, W. J.; Hehre, W. J.; Binkley, J. S.; Gordon, M. S.; DeFrees, D. J.; Pople, J. A. *J. Chem. Phys.* **1982**, 77, 3654–3665.
- (30) Peng, C.; Schlegel, H. B. *Israel J. Chem.* **1993**, 33, 449–454.